Received: 23 April 2019 | Revised: 5 July 2019 | Accepted: 11 July 2019

DOI: 10.1002/er.4762

RESEARCH ARTICLE

WILEY INTERNATIONAL JOURNAL OF ENERGY RESEARCH

Assessment of extreme and metocean conditions in the Maldives for OTEC applications

Giovanni Rinaldi[1] | George Crossley[1] | Ed Mackay[1] | Ian Ashton[1] | Max Campbell[2] | Tim Wood[2] | Lars Johanning[1]

[1] Renewable Energy Group, University of Exeter, Penryn Campus, Penryn, UK

[2] Global OTEC Resources Ltd, Newquay, UK

Correspondence
Giovanni Rinaldi, Renewable Energy Group, University of Exeter, Penryn Campus, Treliever Road, Penryn TR109FE, Cornwall, UK.
Email: g.rinaldi@exeter.ac.uk

Funding information
European Union under the European Regional Development Funding (ERDF) Marine-i, Grant/Award Number: 05R16P00381

Summary

The Maldives is a group of tropical atolls, considered globally to be one of the most desirable holiday destinations. There is an urgent requirement to decrease their dependency on fossil fuels that are currently the main source of energy, and a number of renewable energy alternatives are being evaluated. Among these, due to the favorable oceanographic and bathymetric conditions, ocean thermal energy conversion (OTEC) systems represent a viable opportunity for clean and reliable power. However, the stresses the OTEC platform will need to endure during adverse environmental conditions are not well defined. The magnitude of these stresses will then have a direct influence on the design of the OTEC device. In order to overcome this uncertainty, this paper uses hindcast data sets from global weather and ocean models to assess the metocean conditions of the Maldives, with particular reference to extreme conditions. After selecting a suitable location for the deployment of the devices, return values calculated using the peaks-over-threshold (POT) methodology are estimated for wind, waves, and currents. The 100-year return value for the significant wave height is found to be 4.5 m, with a joint occurrence of energy periods between 7.5 and 8.5 seconds, whereas the 100-year return wind has a velocity of 17.8 m/s and the 100-year return current of 1.9 m/s. The directionality of these extreme events is also considered, showing the southern and western sub-quadrants as the prevailing sources, which provides essential information for positioning of the platform. Additional evaluations of tropical revolving storms (TRS) and variations in temperature and salinity patterns are also provided over a 1500-m water column; temperature varies by approximately 24°C, and salinity by around 2 ppt, showing the suitability of OTEC platforms in the Maldives. This work is therefore of interest to offshore renewable energy stakeholders interested in developing a project in the Maldives or those conducting an analogous analysis in other locations.

KEYWORDS

extreme analysis, OTEC, Maldives, metocean data, TRS

1 | INTRODUCTION

The Maldives is one of the most beautiful archipelagos and holiday destinations of the world. Their territory, which spans over 300 km^2, is mainly constituted of coral reefs and sandy beaches. Despite a relatively small number of inhabitants, due to population growth and the increasing number of tourists, the energy demand is expected to increase significantly in the coming years.[1] Current electricity demand is satisfied primarily by diesel generators, leaving the territory vulnerable to oil price fluctuations and increasing the risk of contamination. To overcome this, the government of the Maldives aims to be carbon neutral by 2020.[2] Hence, a number of clean and renewable power generation methods, and their suitability to the Maldives territory, have been recently explored.

Onshore wind and photovoltaic installations are currently excluded from the energy strategy of the archipelago. This is due to perceived potential for repercussions on tourism from visual and acoustic impacts of these technologies.[2] The focus has therefore shifted to marine energy solutions, characterized by low visual impact on the landscape, scalability, and high suitability to the remote marine environments in this region, especially when land-based alternatives are not viable. The most widely deployed marine energy source worldwide is offshore wind energy, although Elliott et al[3] designated the availability of wind energy to be moderate for large-scale conversion in the Maldives. Contestabile et al[4] performed a wind and wave energy assessment around two locations in the Maldives. The annual offshore wave power was found to range between 8.46 and 12.75 kW/m, while the 10- and 100-m mean wind power density is respectively 0.08 and 0.16 kW/m^2. Although more fundamental research is required to develop a viable technological solution,[5] the authors concluded that combined and colocated offshore wind and wave technologies would be the most promising solution. A study provided in Owen et al[2] considered the use of marine current turbines in the same region, concluding that these would be a suitable alternative to produce electricity by exploiting the monsoonal currents.

Ocean thermal energy conversion (OTEC) is a technology that, through a thermal power cycle combined with a classic vapor turbine, exploits the temperature gradient between the surface and the depths of the oceans, typically to produce electricity.[6,7] Other applications include marine farming, hydrogen production, and desalination of water.[8] Cool bottom water (CBW), found at a depth of 1500 m, is brought to the surface through a deepwater riser. Warm surface water (WSW) is brought on to the platform from a depth of 2 m via a shallow water riser. The WSW and CBW are then passed through respective evaporators and condensers that drive the ammonia system. The efficiency of the OTEC system is dependent on the temperature difference between the WSW and CBW (ΔT). For maximum OTEC system efficiency, a ΔT that exceeds 20°C is desirable. Among the main advantages of this technology are the steadiness of the energy produced, both in terms of its intensity and duration, and the lack of limitations in use of land or intermittency of the resource. On the other hand, a number of technical and socioeconomic limitations related to the construction and deployment of an OTEC plant exist, as detailed in Devault and Péné-annette.[9] Here, OTEC installations are subdivided into land based and floating, and the possible hazards caused by both kinds of projects are investigated. Among these, the most common are possible alterations on the habitat (eg, artificial upwelling of deep water, noise, and electromagnetic fields) and the possible leakage of toxic elements, eg, ammonia, HFC refrigerants, and other compounds.[10] An assessment of the impacts of various effluent discharge methodologies for OTEC applications is provided in Nihous[11] and an evaluation of the large-scale implementation of OTEC systems in Jia et al.[12] In addition, factors like the acceptance of a novel technology, the high capital costs, the competition with other forms of energy, and geographic limitations[8] can limit the development of OTEC.

The use of OTEC systems in the Maldives was until now underexplored, principally due to concerns related to the effectiveness of the technology.[13] However, due to recent technological advances,[14] this application has reached a stage that allows confidence in the production, provided that appropriate conditions are satisfied. As shown later on in this paper, a suitable differential in temperature exists in the marine areas surrounding the Maldives, which, when combined with the urgent requirement to diversify the energy supply, makes OTEC an area of serious consideration for the country.

Thus, despite an holistic approach considering all the above-mentioned aspects is needed to assess the complete viability of an OTEC plant, the main objective of this paper is to provide an assessment of the metocean conditions in support of a feasibility analysis of deploying marine energy infrastructure in the Maldives. The main novelty consists in focusing on the assessment of extreme meteorological events, where large waves or strong winds could damage installed infrastructure, with particular reference to the use of barge OTEC platforms at a specific location in the Maldives. Using historical meteorological model data, extreme values for wind, waves, and currents are calculated. In addition, further factors that can have an impact on the OTEC platforms, such as tropical revolving storms (TRS) and variations in temperature and salinity patterns, are evaluated.

For OTEC, this has important repercussions for the deployment of the platform, especially in terms of positioning, structural requirements, and mooring configuration. Two possible mooring system configurations are usually considered for this kind of application. The first involves a turret system where the OTEC system weather vanes around a mechanical swivel in order to face the prevailing weather. Three mooring lines, each separated by 120°, are attached to the turret. The second possible mooring configuration is a spread mooring where four separate lines, separated at 90°, are connected to the four corners of the barge. The extreme events analysis informs the decision as to which mooring configuration should be selected. It also allows the mooring line tensions to be estimated, as well as the mooring line diameter to be defined.

Based on the return values calculated, optimum values for the design and positioning of the devices are derived. As such, the outcomes of this work are of primary interest to any stakeholder interested in OTEC applications around the Maldives. However, the results also can provide valuable information to device developers and decision makers wishing to install other ocean renewable technologies in the same location. Furthermore, the methodology for including extreme events in feasibility assessment for offshore infrastructure is relevant to generic marine renewable energy projects in other areas.

2 | METHODOLOGY

2.1 | Metocean data

Preliminary site screening considered not only technological but also socioeconomic implications, such as the proximity to tourist resorts. Following this process, the site preselected for this study is around 6 km southeast of Malè Atoll. This location, shown in Figure 1, is not only in the vicinity of the most populated city but also satisfies the depth requirements (approximately 1500 m) for the installation of an OTEC generation platform (needed to reach a sufficient ΔT). Because of the lack of suitable measurements for wind and waves in the regions of interest, the metocean data from this work have been retrieved using hindcast models available in the public domain.[16-19] These models, together with a description of their basic specifications and the data used, are reported in Table 1. Wave and wind reanalysis data sets downloaded through the SOWFIA platform are accessible at http://sowfia.hidromod.com/PivotMapViewer/.[19] Similarly, ERA-Interim reanalysis data sets can be accessed at https://www.ecmwf.int/en/forecasts/datasets/reanalysis-datasets/era-interim[20] and HYCOM data at https://www.hycom.org/dataserver/gofs-3 pt1/reanalysis.[21] The full set of metocean data retrieved for this work can be downloaded through the supporting information provided with this manuscript.

The data from the ERA-Interim model have been compared with those from the WWIII model. The comparison showed that the two data sets are consistent, both in terms of magnitude and directionality, with correlation coefficients of.82 for significant wave height and.70 for wind speed. However, agreement between different models does not ensure that these are reasonably accurate, since these could be affected by performance issues in dynamically difficult regions. Examples of these difficulties can be found in Shanas and Kumar,[23] and examples of how discrepancies can be overcome by means of validation through instrumentation in Sangalugeme et al.[24] Therefore, in the absence of suitable instrumentation data, in order to obtain a basic validation of the retrieved data, as well as preliminary indications of the phenomena characterizing the area, the results derived from these data set have been compared against information available in literature. Specifically, the wind and waves distributions have been compared against the results published in Contestabile et al,[4] and similarity between results added confidence to the accuracy of the WWIII data. Similarly, the currents and temperature distributions have been compared against the results published in Lüdmann et al.[25] Also, in this case, the data sets provide information consistent with the outcomes provided in the publication, indicating the regional oceanographic setting dominated by the Indian monsoons, with values of current up to 1 m/s, and the local current regime of the Maldives mainly influenced by wind-induced surface currents. Finally, the sea surface salinity has been compared with the results in Rao and Ram[26] indicating averages of 34 to 36 psu.

Because of the finer spatial and temporal resolution of the WWIII data retrieved using the SOWFIA platform, these have been used for the subsequent evaluations and extreme values analysis. The HYCOM + NCODA Global 1/12° Analysis provides five variables, namely, sea surface height, eastward velocity, northward velocity, in situ temperature, and salinity at 40 vertical depth levels ranging from 0 m at the ocean surface to 5000 m. The metocean data retrieved from the HYCOM database are collected during a shorter period due to restrictions on the data available.

The current speeds estimated in this model do not include the tidal forcing components, being therefore representative of the ocean currents only.[22] However, from preliminary analysis in the same region,[25,27,28] it can be asserted that deeper currents (below 200 m) are probably derived by Kelvin Waves and Rossby Waves, as well as that tidal ranges are about 0.7 to 1 m with tidal forcings

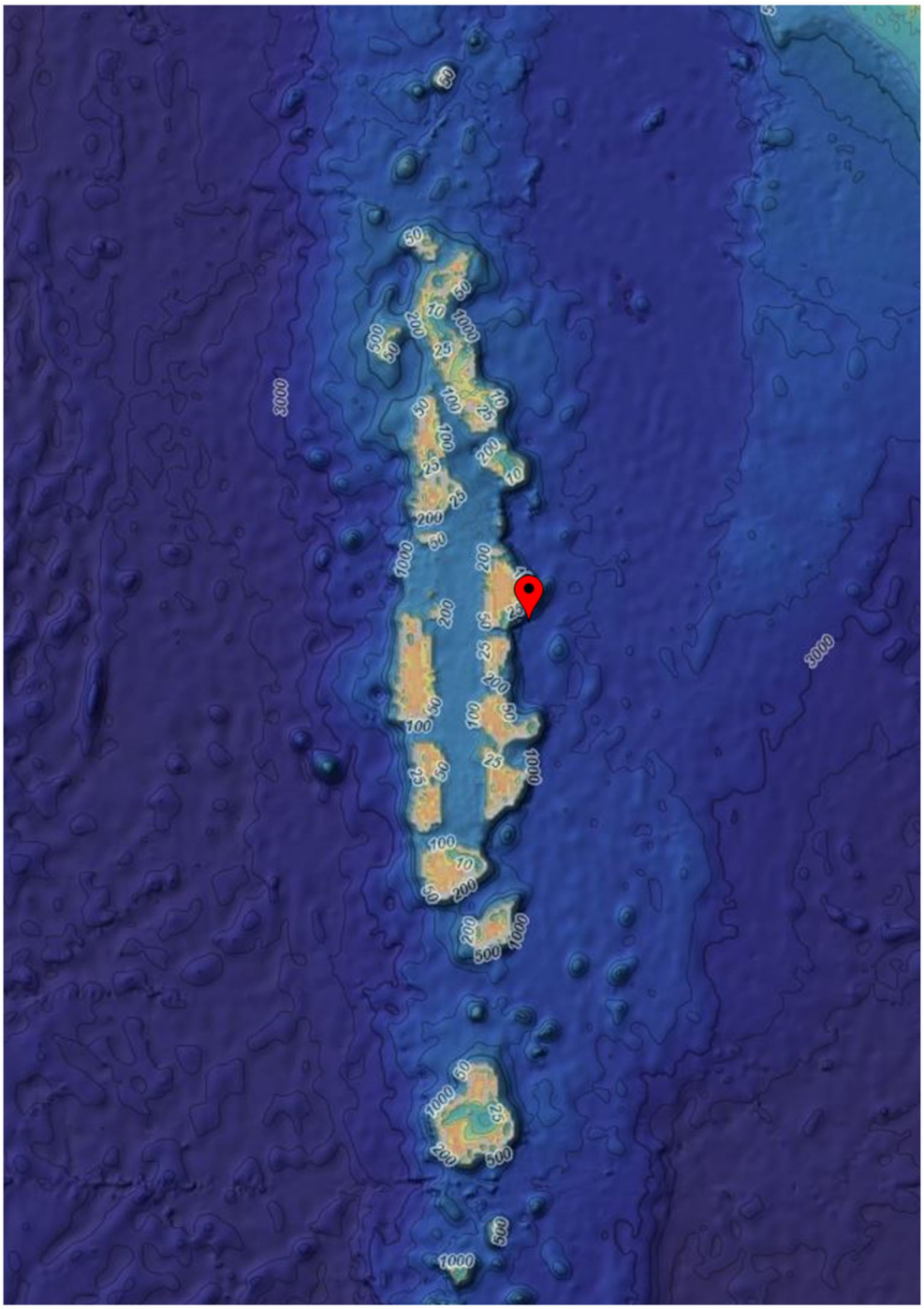

FIGURE 1 Map of the Maldives with pin on the investigated location. Coordinates: 4°16′N, 73°37′E. Retrieved from the National Oceanic and Atmospheric Administration[15] [Colour figure can be viewed at wileyonlinelibrary.com]

affecting mainly the narrow channels between atolls. Finally, the current speed is retrieved for a depth of 0 m (ie, the water surface).

2.2 | Extreme value analysis

The prediction of extreme values is a key consideration in the design of offshore infrastructure. Estimating the likelihood and intensity of long-term extreme events ensures that not only safety conditions are met but unnecessary costs of overengineering the structure are also saved. For these reasons, models for extremes, which permit extrapolation beyond the values available in a data set, are often used to characterize events recurring only at sporadic intervals.

Extreme values can be computed by means of standard distribution functions, provided that these are matched

TABLE 1 Summary of the models used to retrieve the metocean data and their basic properties

Model/ Data Set	Institute/ Platform	Parameters Obtained	Length of Time (Period)	Frequency (Time Step)	Spatial Resolution
Wavewatch III (WWIII)	SOWFIA[16,19]	Significant wave height (H_S), energy period (T_E), wind speed, wind direction, wave direction	30 years (1979-2008)	3 hours	0.5° (~55 km)
ERA-Interim	ECMWF[17,20]	Significant wave height (H_S), energy period (T_E), wind speed, wind direction, wave direction	30 years (1979-2008)	6 hours	0.75° (~80 km)
HYCOM	NOPP[18,21,22]	Current speed, current direction, temperature, salinity	21 years (1994-2014)	3 hours	0.08° (~9 km)

Abbreviation: ECMWF, European Centre for Medium-Range Weather Forecasts.

with extreme values samples derived from the set of data available and certain requirements (eg, independency and homogeneity of the extremes) are satisfied.[29] A number of methods, for both short-term and long-term extremes predictions, are currently available in extreme value literature.[29-32] The peaks-over-threshold (POT) method is chosen in this work to estimate extreme wave, wind, and current conditions in the Maldives. This method is the most commonly used in extreme waves analysis; it does not require assumptions about the distribution of the bulk of the data and uses more data than methods such as the annual maximum method, leading to lower uncertainty in the estimates of return values.[33-37]

The POT method is based on the asymptotic result that for any "well-behaved" distribution, the conditional distribution of independent exceedances of a high enough threshold tends to the generalized Pareto distribution (GPD).[29] In practice, observations of environmental variables such as winds, waves, and currents exhibit significant serial correlation and are not independent. However, the requirement that threshold exceedances are independent can be met by only modelling the peak values in storms separated by a sufficient time that the peak values are effectively uncorrelated. In the present analysis, storm peaks are defined as any values that are a local maximum within a 5-day window. This separation time corresponds approximately to the time taken for a pressure system to pass, meaning that discrete storm peak values should correspond to different generating systems. (A separation criterion of 5 days can be justified more rigorously by considering the correlation between adjacent storm peaks—see, eg, Mackay and Johanning[38]). Alternatively, specific algorithms like the one presented in Soukissian et al[39] can be used to determine the appropriate time separation interval for each data set.

A suitably high threshold must also be selected, above which the asymptotic model is assumed to be valid. A high threshold leads to the asymptotic model being more appropriate and reduces bias in the estimates. However, a higher threshold also leads to fewer data being available for use in the inference, which results in greater variance in the estimates. The choice of threshold is therefore a trade-off between bias and variance. Normally, the threshold is selected by fitting the GPD for a range of threshold values and selecting the threshold as the lowest value for which the GPD shape parameter and estimated return values tend to stable values.[29] This method has been used in the present work.

Return values and return periods are defined in terms of the distribution of storm peaks significant wave height, H_s^{SP}, as follows.[29,38] If $\Pr\left(H_S^{SP} \le h \middle| H > u\right)$ is the probability that H_s^{SP} does not exceed the height h, given that H_S^{SP} exceeds the threshold value u, then the T-year return value of the significant wave height H_T is defined as the solution of the following:

$$\Pr(H_S > H_T | H > u) = {}^{1}/_{Tm}, \quad T > \frac{1}{m}, \tag{1}$$

where m is the expected number of threshold exceedances per year and T is referred to as the return period and is the average time between exceedances of H_T. In this way, return periods and return values are calculated. These can then be used as design parameters for the investigated system, eg, an offshore structure.

For data above the threshold, the range of periods is estimated by considering the wave steepness. For deep waters, this is calculated as follows[33]:

$$s_e = \frac{H_S}{\lambda_e} = \frac{2\pi H_S}{gT_e^2}, \tag{2}$$

where H_S is the significant wave height, λ_e is the wavelength and T_e the energy period.

3 | RESULTS

3.1 | Climate analysis

In order to obtain an overview of the metocean conditions at the selected location, the wind, wave, and current distributions are analyzed. The direction-intensity histogram ("rose") together with bivariate histograms, for wind, waves, and currents is provided according to the data produced with the WWIII and HYCOM models. The results of this initial analysis are shown in Figures 2–8. The significant wave height varies between 0.1 and 5 m, with the most frequently occurring value around 1.2 m (Figure 2). The energy period distribution shows values up to 20 seconds, with the peak of the distribution at around 8 seconds (Figure 3). Most of the wave resource comes from the southeast quadrant, which can be explained by the position of the investigated site with respect to the surrounding atolls (Figure 1).

The most common wind speed is around 6 m/s, with a maximum observed value of 18 m/s (Figure 5). In terms of directionality, the wind is predominantly coming from the western quadrants. Since the two have distinct forcing, the dominant wind direction cannot be directly compared against the peak spectral wave direction shown in Figures 2 and 3. Besides, as anticipated from the analysis in Contestabile et al,[4] the energy patterns suggest that wind and waves are generally uncorrelated, especially during the period of southwest monsoon.

The peak of the surface current speed distribution (mean value) is around 0.45 m/s, with very few occurrences of values up to 2 m/s (Figure 7). Since the effects of tidal forcing are not included in the database consulted, the analyzed currents are modelled as driven and affected by thermodynamical and biochemical processes.[18] Two different sectors of provenance (west and southeast) can be mainly identified when their directionality is analyzed (Figure 7).

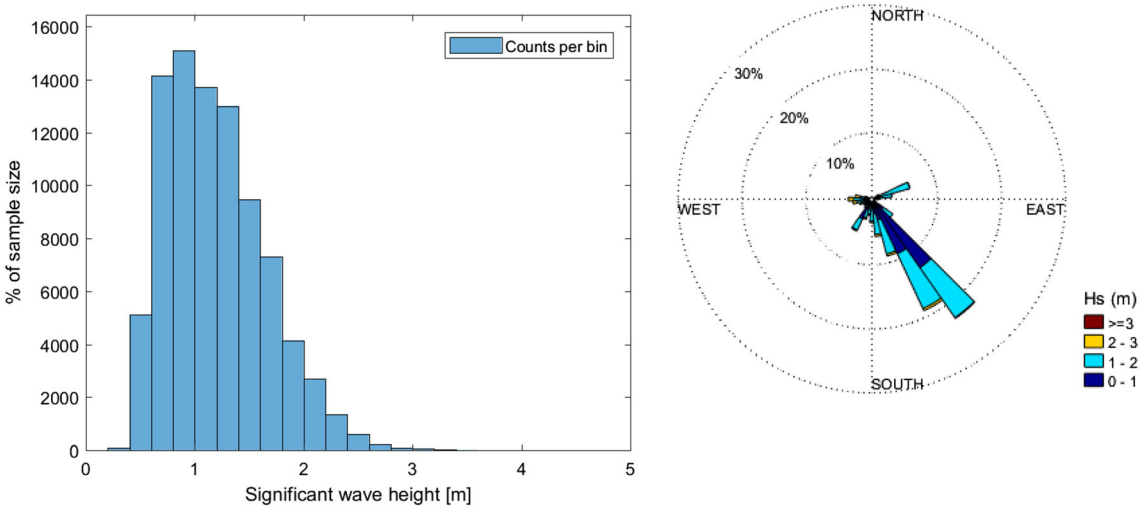

FIGURE 2 Distribution and rose of significant wave height [Colour figure can be viewed at wileyonlinelibrary.com]

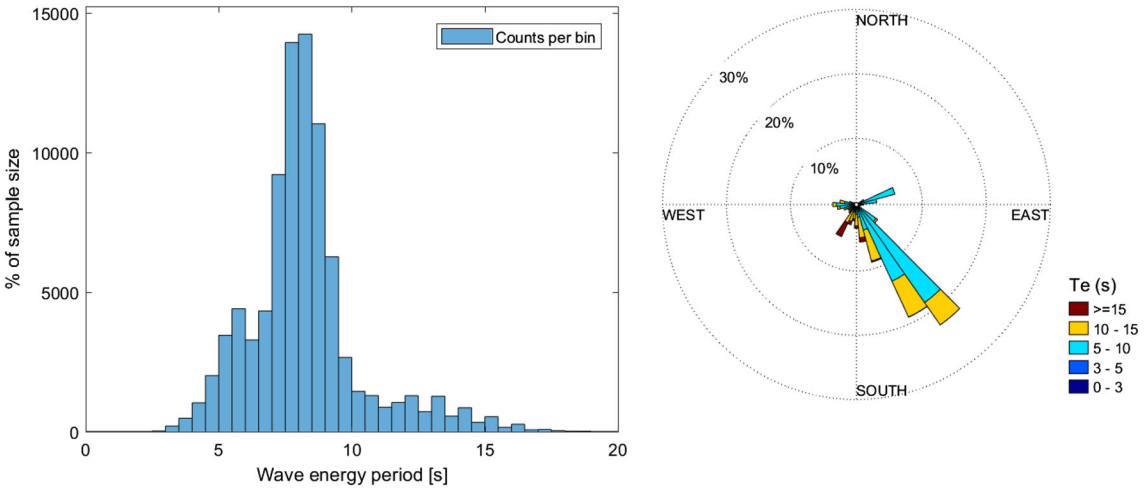

FIGURE 3 Distribution and rose of wave energy period [Colour figure can be viewed at wileyonlinelibrary.com]

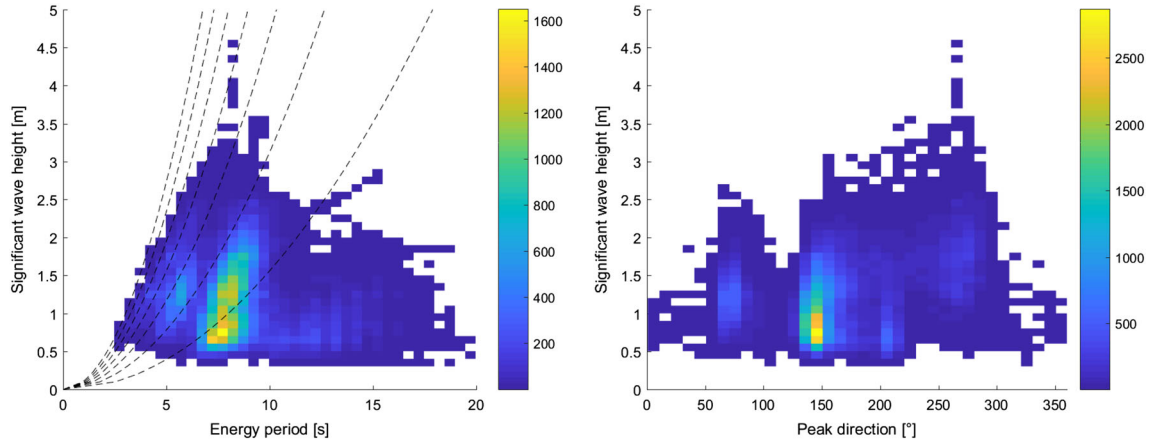

FIGURE 4 Bivariate histogram of significant wave height and energy period (left) and of significant wave height and peak direction (right). Color scale denotes percentage of sample size in bins of size 0.1 m by 0.5 s and 0.5 m by 10°, respectively. Black dashed lines indicate constant steepness (values between 0.01 and 0.07) [Colour figure can be viewed at wileyonlinelibrary.com]

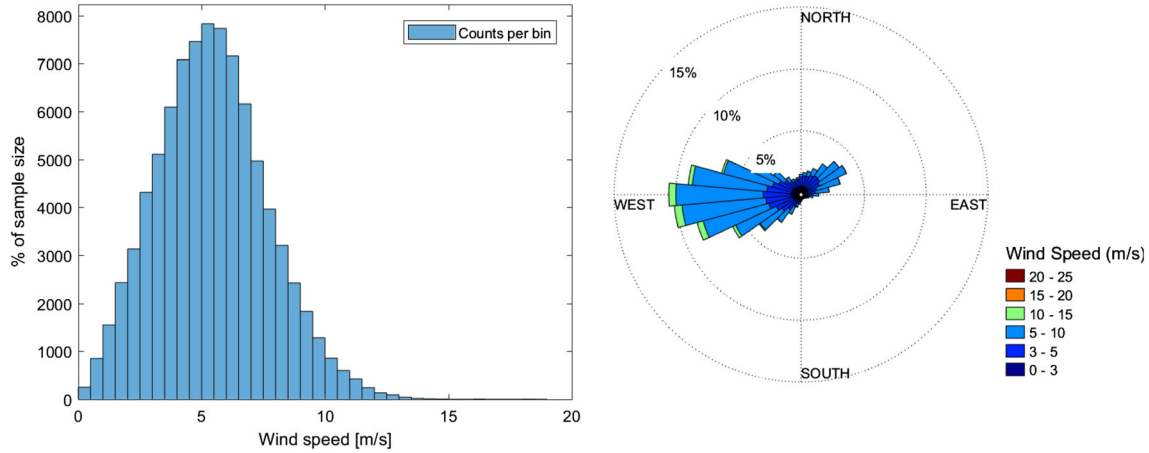

FIGURE 5 Distribution and rose of wind speed [Colour figure can be viewed at wileyonlinelibrary.com]

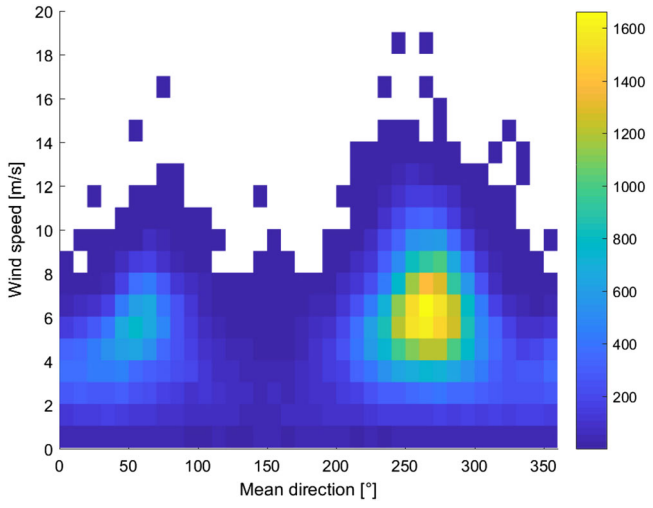

FIGURE 6 Bivariate histogram of wind speed and mean direction; color scale denotes occurrence in bins of size 1 m/s by 10° [Colour figure can be viewed at wileyonlinelibrary.com]

3.2 | Extreme values

Once a preliminary overview of the climate in the selected location is obtained, the extreme value analysis is performed using the POT method over wave, wind, and current resource.

A minimum separation of 5 days is chosen as an appropriate interval between two consecutive extreme events, in order to ensure independency between them, for wind and waves. However, this interval is reduced to 1 day for the extreme currents, based on the assumption that nontidal-driven currents vary on a shorter timescale, and is therefore easier to hypothesize independency between two consecutive extremes in a shorter period.

This gave 834 peaks for the significant wave height, 901 for the wind speed, and 2464 for the current speed. A number of 1000 bootstrap trials are run in order to support the threshold selection by randomly resampling the

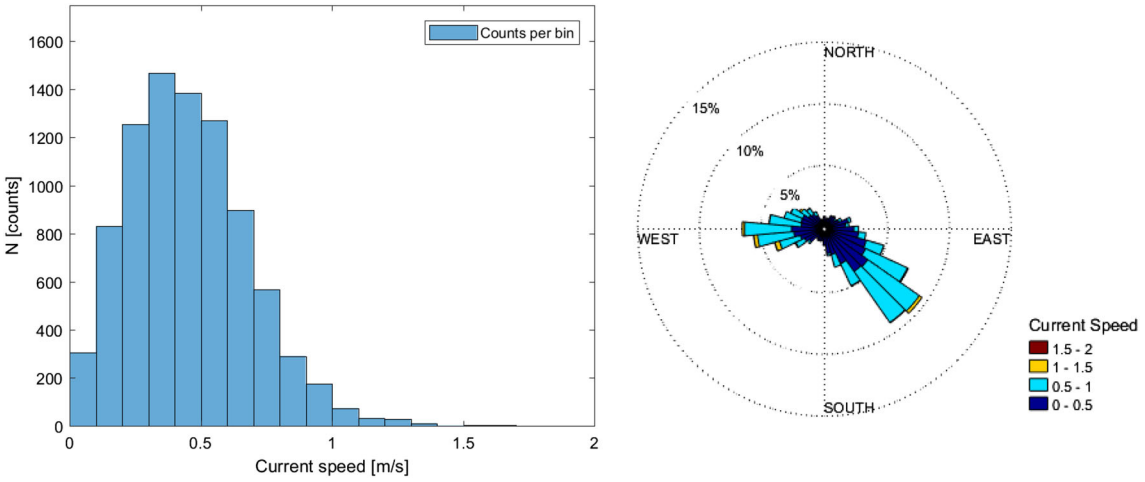

FIGURE 7 Distribution and rose of current speed [Colour figure can be viewed at wileyonlinelibrary.com]

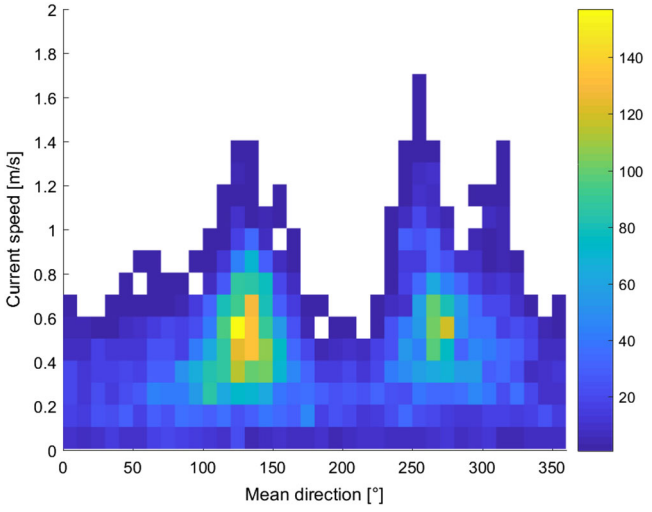

FIGURE 8 Bivariate histogram of current speed and mean direction; color scale denotes occurrence in bins of size 0.1 m/s by 10° [Colour figure can be viewed at wileyonlinelibrary.com]

data. The maximum value for each vector of thresholds is selected when 15 peaks or less remain above that value.

An example of plots for threshold selection is provided in Figure 9, in which the 50-year return period is used to aid in the identification of a suitable value. From the plot in this figure, the threshold has been arbitrarily selected as 2.4 m due to the relative stability of shape parameter and return values after this value.

After selection of a suitable threshold, estimates of the GPD parameters are found using the empirical Bayesian method of Zhang.[40] The selected threshold values for significant wave height, wind speed, and current speed were 2.5, 12.1, and 0.7 m/s, respectively.

The results of this analysis are shown in Figure 10. Return values for the energy period are not extrapolated on their own, since the longest period waves are relatively low (see Figure 4) and these are less relevant for the

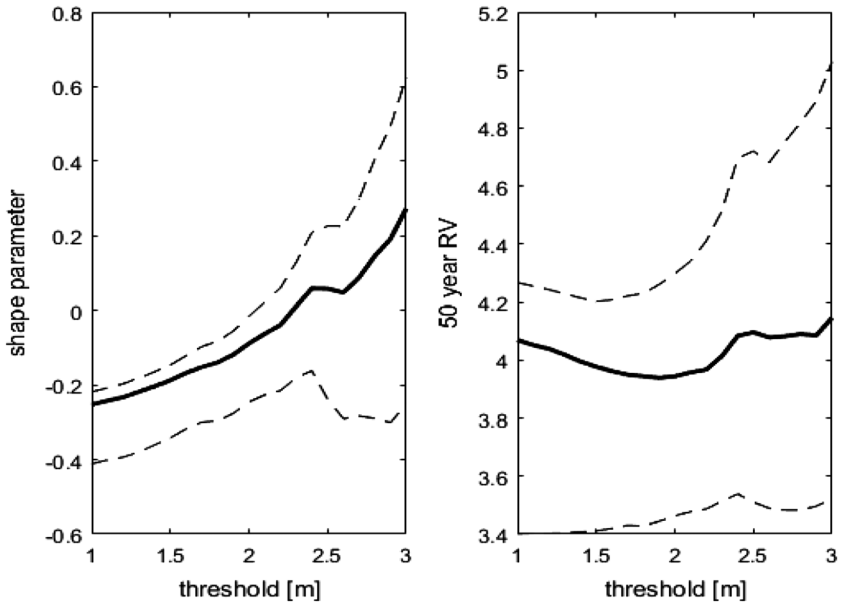

FIGURE 9 Example of plots for threshold selection (for significant wave height)

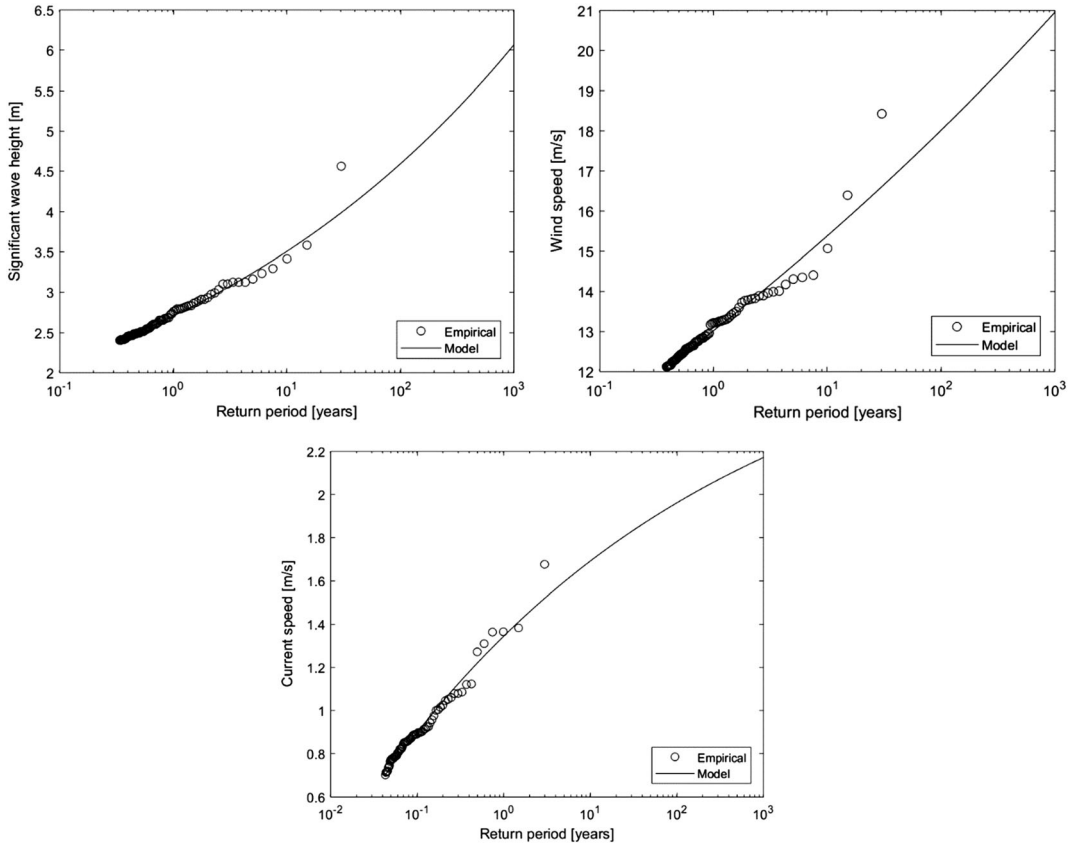

FIGURE 10 Results of the extreme value analysis for the selected location. Return values are plotted as a function of the return periods for significant wave height (top left), wind speed (top right), and current speed (bottom)

design of offshore structures.[41] Therefore, the analysis focuses on estimating the extremes significant wave height and associated wave periods. For each return value of the significant wave height, the associated range of return periods is provided by selecting the minimum and maximum energy period observed the estimated return value for significant wave height. If the return value is above the observed data, the constant steepness projections, introduced in the previous section, are used to estimate the possible range of associated periods. An example of this range estimation is provided in Figure 11. In this figure, 4.8 to 7.5 seconds and 5.5 to 6.3 seconds are provided as suitable associated ranges for the 1-year (1.83 m) and 10-year (2.43 m) return values; however, the range 6.7 to 9.5 seconds has to be estimated by means of the constant steepness projections for the 100-year return value (2.86 m).

The modelled distributions provide a good fit for the values sampled from the climate models described in Section 2.1, allowing for extrapolation beyond these. The 100-year return value for the significant wave height is 4.5 m, with a joint occurrence of energy periods between 7.5 and 8.5 seconds, whereas the 100-year return wind has a velocity of 17.8 m/s and the 100-year return current of 1.9 m/s. These extreme values have been calculated

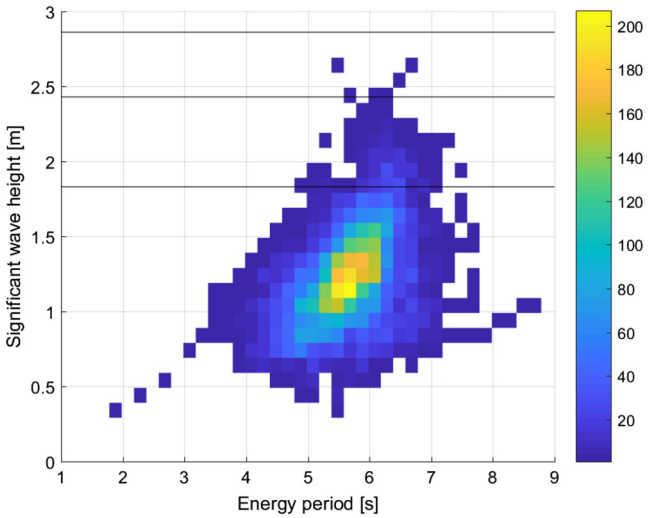

FIGURE 11 Bivariate histogram of significant wave height and energy period for the east subsector; color scale denotes percentage of sample size in bins of size 0.1 m by 0.2 s. Black lines indicates 1-, 10-, and 100-year return values for the subsector (1.33, 2.08, and 2.47 m, respectively) [Colour figure can be viewed at wileyonlinelibrary.com]

with a 95% confidence interval, estimated using the bootstrap technique.[33,38] Confidence bounds (2.5% and 97.5% quantiles) are as follows: (3.5-5.8 m) for the 100-year

return waves, (14.6-21.8 m/s) for the 100-year return wind, and (1.6-2.8 m/s) for the 100-year return currents.

In addition to the omnidirectional extreme values estimation for the selected location, a further characterization is sought in order to derive indications on the optimum positioning of the device. Hence, the initial data set is subdivided in eight directional sectors, as shown in Figure 12, according to the direction of each measurement. The range for the subdivision is the same for all variables (wind, waves, current). For convenience, the directional extreme values obtained after this subdivision, together with each angular range, percentage, and number of associated values, and selected threshold values are collected in Tables 2–4. A range of possible associated energy periods is provided for each extreme value according to the data in that subsector. The confidence bounds for these return values are provided in Appendix A, Tables A1–A3.

The relationship between significant wave height and steepness for the entire data set exploited in this study is shown in Figure 13.

When the directional extremes are analyzed, the empirical distributions vary with the direction and, therefore, also the fitted distributions for the extreme events calculation (Figure 14). The results of this directional analysis indicate that the most energetic waves (highest height and period), as well as the most extreme winds and currents, all come from the southwest subsectors. This is critical information to determine the orientation of the platform. For some of the subsectors (north and northwest), the extreme waves could not be extrapolated due to the scarcity of values among the retrieved metocean data, which makes the fitting of a probability distribution unattainable.

3.3 | Tropical revolving storms

Because of their position, the Maldives could be subject to dangerous extreme events resulting from TRS, also known as cyclones or severe cyclonic storms. These low-pressure perturbations not only can last up to weeks and bring direct implications for the population, eg, flooding or tsunamis, but also present important risks for any structure installed in the proximity of the storm.[42]

Tropical cyclones are characterized by sharp gradients of pressure and present a coupling between the thermodynamics of the precipitation and the larger scale

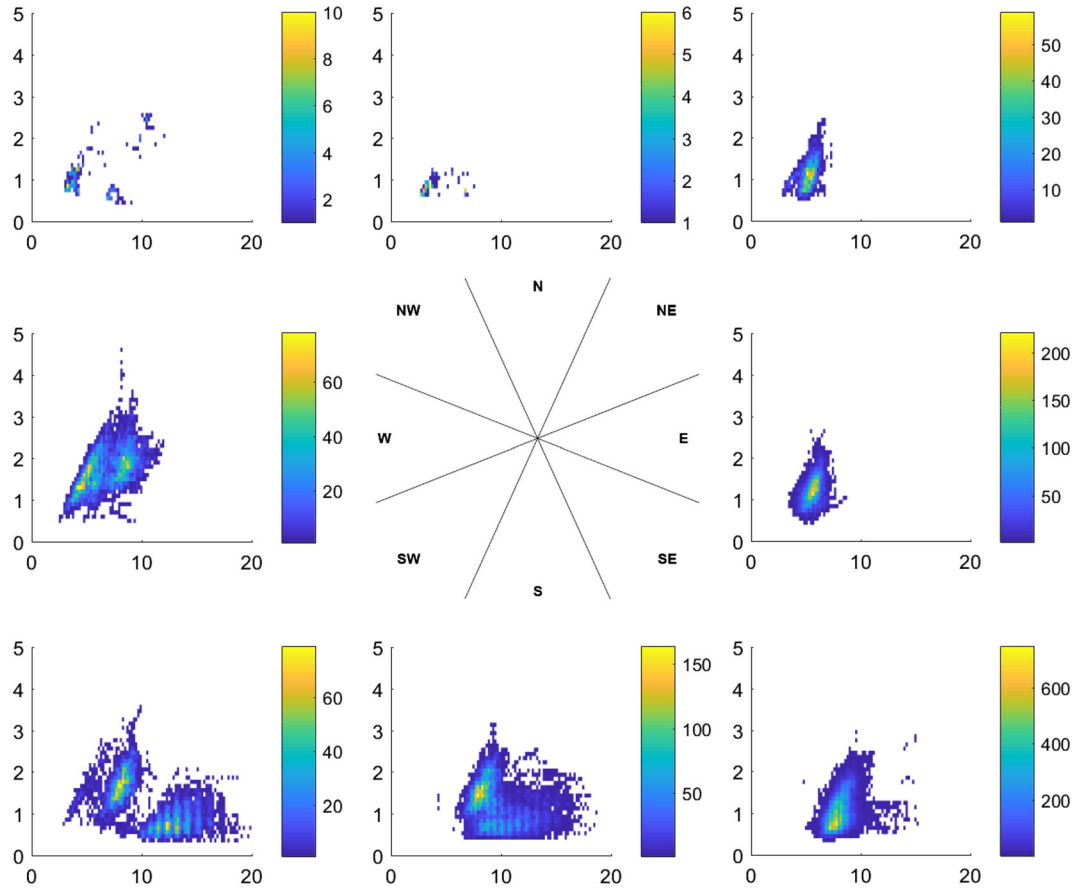

FIGURE 12 Bivariate histograms of significant wave height (on the y-axis, in meter) and energy period (on the x-axis, in seconds) for the different subsectors. Color scale denotes percentage of sample size in bins of size 0.1 m by 0.2 s. The sub-quadrants considered for the directional extreme values investigation are shown in the center

TABLE 2 Directional extreme values for waves in the investigated location

Sector	Angle Range, °[a]	Number of Values	Percentage of Values	Selected Threshold, m	1 year		10 years		100 years	
					H_S, m	T_E[b], s	H_S, m	T_E[b], s	H_S, m	T_E[b], s
N	337.5-22.5	78	0.09	-	-	-	-	-	-	-
NE	22.5-67.5	2033	2.34	1.4	1.34	4.2-7.4	2.07	5.2-6.5	2.47	6-6.8
E	67.5-112.5	7689	8.93	1.7	1.83	4.8-7.5	2.44	5.5-6.3	2.82	6.7-9.5
SE	112.5-157.5	42 279	48.29	1.9	1.81	7.1-11.1	2.37	8.7-11.3	2.84	9.5-15.1
S	157.5-202.5	16 863	19.25	2	2.03	7.4-15.2	2.58	8-13.4	3.32	8.3-10.3
SW	202.5-247.5	9093	10.39	1.7	1.89	5-18.8	2.95	8.2-9.4	3.41	9.6-10.1
W	247.5-292.5	9181	10.47	2.2	2.64	5.8-11.2	3.45	7.8-9.7	4.22	8-8.3
NW	292.5-337.5	209	0.24	-	-	-	-	-	-	-

[a]Convention: 0° = North; 90° = East; 180° = South; 270° = West.

[b]Associated range of T_E.

TABLE 3 Directional extreme values for wind in the investigated location

Sector	Angle Range, °[a]	Number of Values	Percentage of Values	Selected Threshold, m/s	1 year	10 year	100 year
					Wind Speed, m/s	Wind Speed, m/s	Wind Speed,m/s
N	337.5-22.5	5782	6.63	5.5	6.70	8.76	9.53
NE	22.5-67.5	12 078	13.95	7.6	9.28	11.72	13.65
E	67.5-112.5	6003	6.91	8.1	9.01	12.46	15.85
SE	112.5-157.5	1138	1.30	4.1	0.91	9.03	12.47
S	157.5-202.5	1883	2.15	5.9	5.14	8.68	9.84
SW	202.5-247.5	14 287	16.30	8.4	11.48	15.19	17.70
W	247.5-292.5	36 439	41.57	9.7	12.87	15.51	17.33
NW	292.5-337.5	9815	11.20	7.3	9.90	12.96	14.33

[a]Convention: 0° = North; 90° = East; 180° = South; 270° = West.

TABLE 4 Directional extreme values for currents in the investigated location

Sector	Angle Range, °[a]	Number of Values	Percentage of Values	Selected Threshold, m/s	1 year	10 year	100 year
					Current speed, m/s	Current speed, m/s	Current speed, m/s
N	337.5-22.5	289	3.36	0.3	0.56	0.74	0.78
NE	22.5-67.5	454	5.29	0.3	0.68	0.93	1.03
E	67.5-112.5	1089	12.68	0.4	0.82	0.94	0.99
SE	112.5-157.5	2869	33.40	0.5	1.19	1.36	1.45
S	157.5-202.5	587	6.83	0.3	0.79	1.01	1.08
SW	202.5-247.5	587	6.83	0.4	0.84	1.40	1.93
W	247.5-292.5	1892	22.03	0.5	1.32	1.65	1.82
NW	292.5-337.5	823	9.58	0.3	1.05	1.38	1.53

[a]Convention: 0° = north; 90° = east; 180° = south; 270° = west.

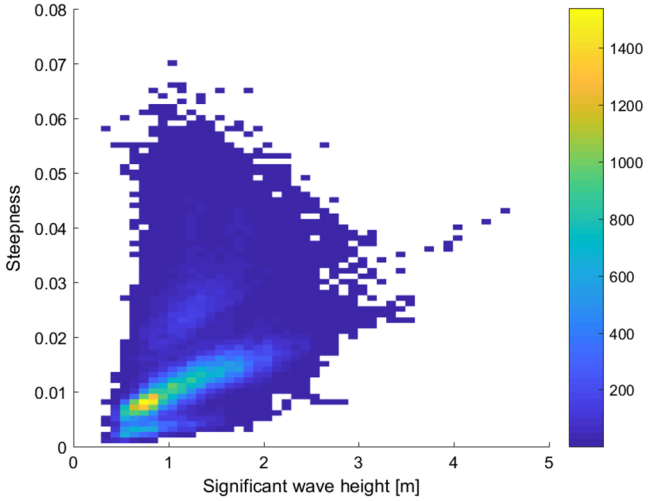

FIGURE 13 Bivariate histogram of steepness and significant wave height; color scale denotes percentage of sample size in bins of size 0.01 m by 0.1 m

structure of the storm. This means that global models struggle to capture the formation and evolution of these events.[43] An alternative is to make use of tools that keep track of past events and the occurrence of storms in the world. One of them, freely available on the European Centre for Medium-Range Weather Forecasts (ECMWF) website,[44] was consulted to find records of those affecting the Maldives area, with the intent of identifying possible patterns and provide recommendations for future events (Figure 14).

This tool provides charts of cyclones tracks since 2011, subdivided by region for five major areas of the world. From this tool, the cyclones affecting the Maldives are selected and collected. Out of the 73 cyclones tracked in the region of interest ("05 - New Delhi"), only 4 of them were registered through the Maldives or the southern coast of India, as shown in Figure 15. Observation lifetimes for each storm are provided in Table 5. The dots indicate the path of the storm, with colors indicating its intensity according to the following terminology[45]:

- TD (1) = Tropical depression: A tropical cyclone with the maximum sustained winds of 33 knots (17.1 m/s, 61 km/h) or less near the center.
- TS (2) = Tropical storm: A tropical cyclone with the maximum sustained winds of 34 knots (17.2 m/s, 62 km/h) to 47 knots (24.4 m/s, 88 km/h) near the center.
- STS (3) = Severe tropical storm: A tropical cyclone with the maximum sustained winds of 48 knots (24.5 m/s, 89 km/h) to 63 knots (32.6 m/s, 117 km/h) near the center.

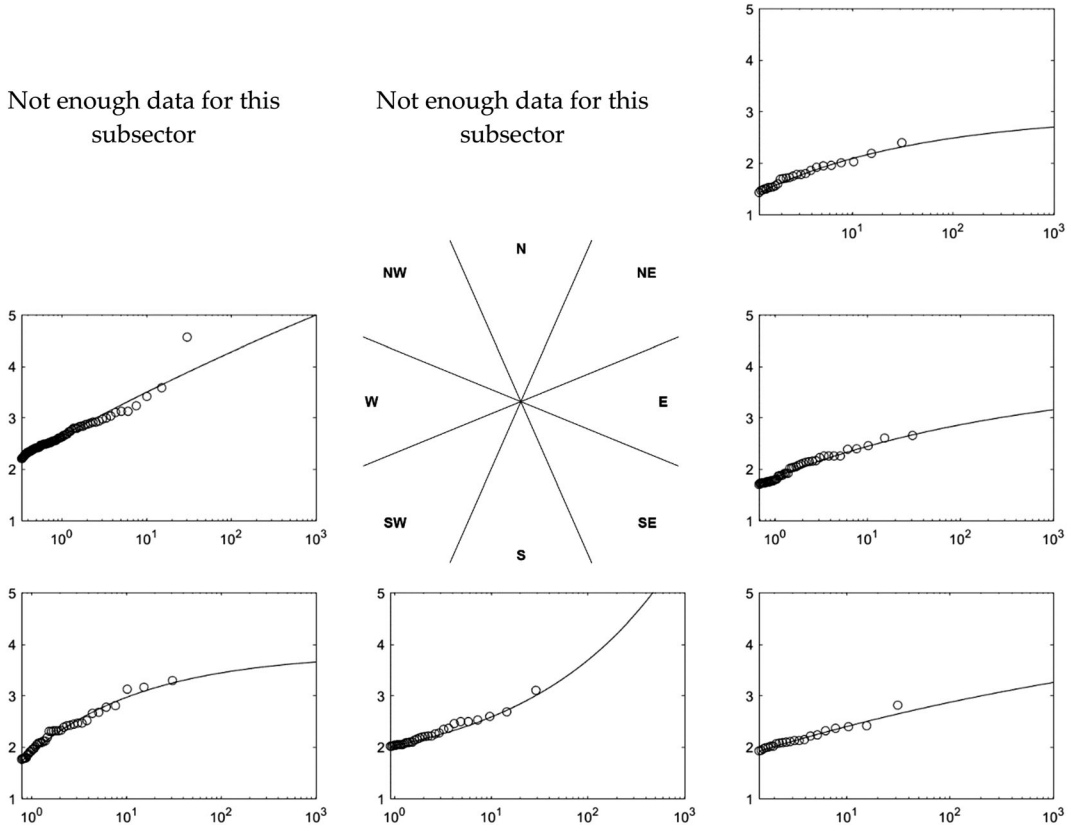

FIGURE 14 Results of the extreme value analysis for the different subsectors. Return values are plotted for significant wave height (on the y-axis, in meter) as a function of the return periods (on the x-axis, in years). The sub-quadrants considered for the directional extreme values investigation are shown in the center

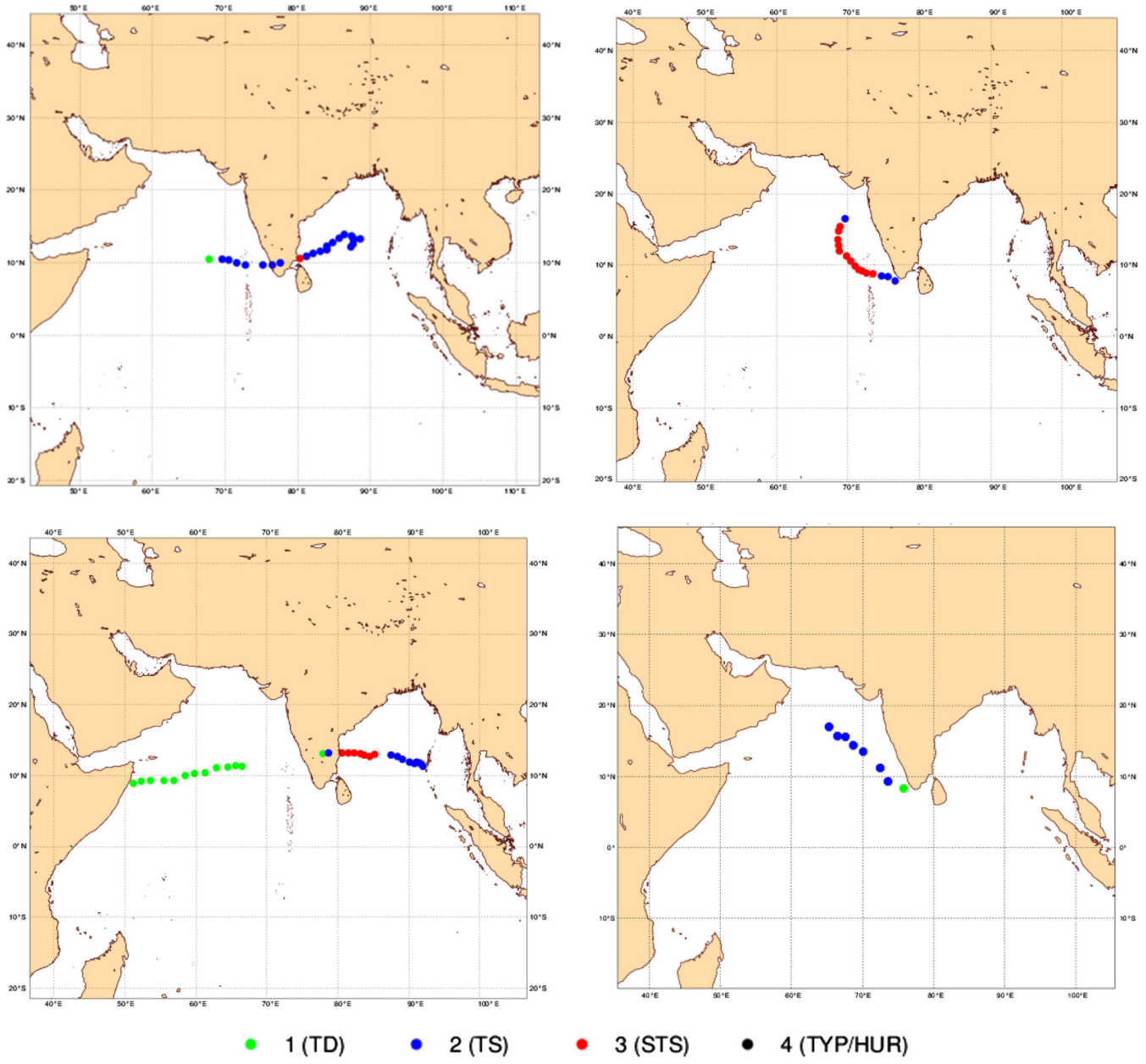

FIGURE 15 Track of past tropical storms registered in the proximity of the Maldives using the European Centre for Medium-Range Weather Forecasts (ECMWF) tropical cyclone track.[44] The colors show the evolution and intensity variation [Colour figure can be viewed at wileyonlinelibrary.com]

TABLE 5 Observation lifetimes for past tropical storms registered in the proximity of the Maldives

Storm Name (as indicated in ECMWF[44])	Observed	
	From	To
Gaja (07B)	11/11/2018	18/11/2018
Ockhi (03B)	29/11/2017	06/12/2017
Vardah (05B)	08/12/2016	19/12/2016
05A (05A)	26/11/2011	29/11/2011

Abbreviation: ECMWF, European Centre for Medium-Range Weather Forecasts.

- TYP/HUR (4) = Typhoon/hurricane: A tropical cyclone with the maximum sustained winds of 64 knots (32.7 m/s, 118 km/h) or more near the center.

Of the four registered events in the period 2011 to 2019, none of them reached the worst classification of typhoon, and all of them can be classified as tropical storms (maximum winds of 88 km/h near the center) or less dramatic events. Their duration was between a day and a week. However, all the tracked events pass through the southern coast of India, barely affecting the Maldives.

In order to extend the period of investigation to events past 2011 and focus the analysis of TRS in the Maldives territory, the cyclones reported in the International Best Track Archive for Climate Stewardship (IBTrACS)[46] have been analyzed. This database, considered by the World Meteorological Organization (WMO) as the official archiving and distribution resource for tropical cyclone best track data, combines information from different data sets to provide a global set of historical cyclones between the years 1848 and 2019. Cyclones are described in terms of the basin where they were registered and their coordinates provided together with measures of wind speed and pressure in a resolution of 0.1° (around 11 km). The results of this analysis for a portion of the Indian Ocean are shown in Figure 16. Here, despite some differences with the previous database, it can be seen how most of the cyclones are concentrated near the southern coast of India or in the middle of the Indian Ocean, with few events of low to moderate intensity directly affecting the Maldives.

In order to focus the cyclones investigation in the region of interest, a rectangular area delimited by a distance of 500 km around the Maldives is defined as detailed in Table 6. Subsequently, the cyclones reported in this database for this area have been isolated and their properties analyzed. A total of 19 cyclones, between 1930 and 2013, is identified in the selected area of interest (which is smaller compared with the one considered for the analysis using the ECMWF model). Values of wind speed retrieved with IBTrACS range from 7 to 29 m/s (with values missing for three cyclones), whereas values of pressure are similar between different events, with values ranging from 996 to 1007 mb. According to the above classification, only one of the cyclones registered with this database reaches the grade of severe tropical storm (29 m/s), and only another that of tropical storm (23 m/s). The 14 remaining ones (excluding those for which wind speed values are missing) are tropical depressions with a maximum wind speed below 16 m/s.

3.4 | Temperature and salinity

The capabilities of the HYCOM model in simulating water temperature and salinity profiles have been demonstrated in different studies.[22,47] However, using this model, the data at the chosen location could be retrieved for a depth up to 700 m. For this reason, data collected by means of conductivity, temperature, and depth (CTD) devices, capable of measuring temperature and salinity through the water column, were used for these characterizations. Similar to the previous data, also these data are extracted from public sources.[48,49]

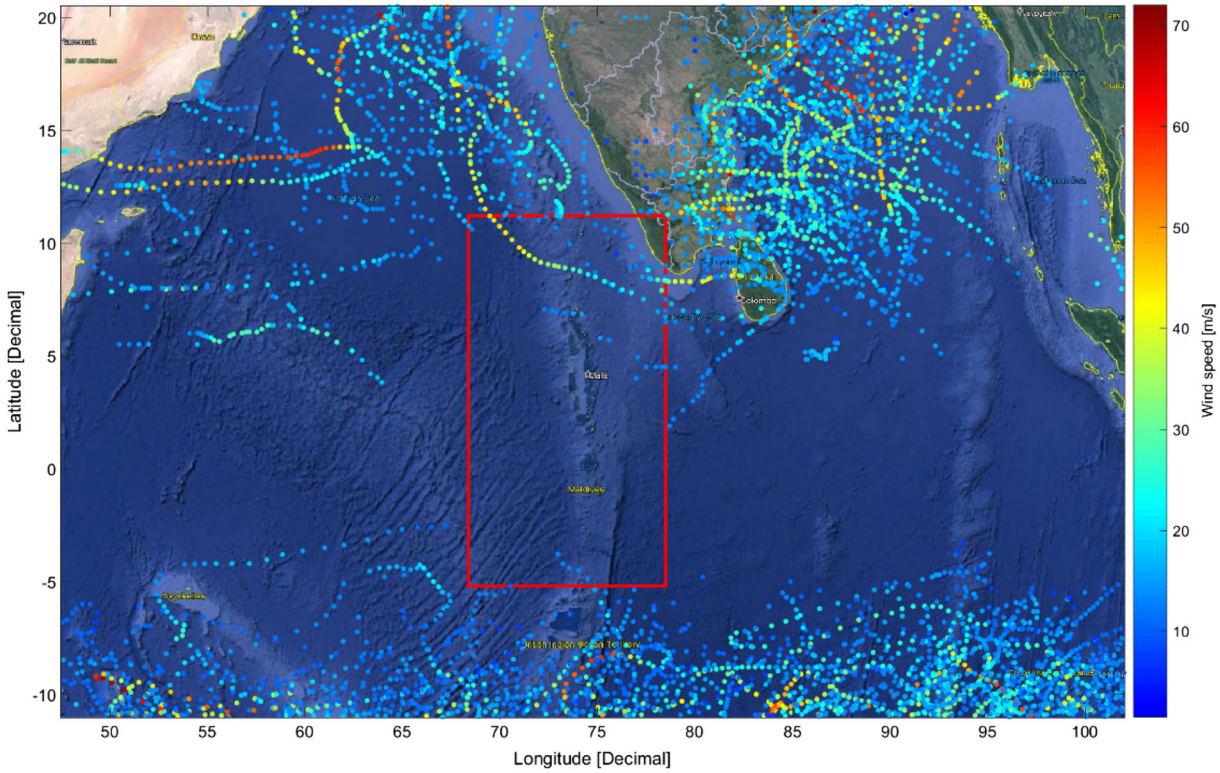

FIGURE 16 Map of the cumulative tracks of all tropical cyclones during the 1848 to 2019 time period in the Indian Ocean using the International Best Track Archive for Climate Stewardship (IBTrACS) tropical cyclone track. The red rectangle refers to the area selected for further investigation [Colour figure can be viewed at wileyonlinelibrary.com]

TABLE 6 Coordinates of the points delimiting the area of 500 km around the Maldives selected for further investigation of TRS with the IBTrACS database

Delimiting Point	Coordinates (Latitude, Longitude)
Northeast	11.2, 78.5
Southeast	−5.2, 78.5
Southwest	−5.2, 68.4
Northwest	11.2, 68.4

Abbreviations: IBTrACS; International Best Track Archive for Climate Stewardship; TRS, tropical revolving storms.

Figure 17 shows both temperature and salinity for three months (June, September, and December), acquired from two separate cruises as single CTD casts, over a depth range 0 to 2100 m at a location 150 km southeast of the Malè Atoll in the Maldives. This constitutes a limitation in the assessment because the selected OTEC site is 144 km away from this location, and bathymetry gradients or other factors may induce variations in the profiles for the two sites. In order to reduce this uncertainty, the temperature profile has been qualitatively compared with that provided in Lüdmann et al[25] obtained through sound velocity profiles, which indicated comparable values and variations. Temperature is reported in degrees Celsius, salinity in parts per thousand (ppt). Temperature data are particularly important, as it will determine the yield of an OTEC device as well as the required riser depth. Salinity is less relevant than temperature but is required in designing the device's pump and riser specs.

Salinity and temperature vary most in the top 200 m of the water column. Variation over the year is small, although some variation is noted corresponding to the tropical seasonality common of this region. Water temperature throughout the entire depth varies by approximately 26°C, with salinity ranging around 0.7 ppt over the year and less than 2 ppt through the water column. Over a depth of 1500 m, typical of OTEC concepts, a temperature range of about 24°C is achieved.

4 | DISCUSSION

The findings of the previous section can be analyzed in the broader context of metocean climate characterization, as well as in their specific relevance to extreme events and OTEC applications in the investigated location.

Starting from the long-term distribution of significant wave heights, it can be seen how the wave resource is relatively low if compared with typical values in other areas of the Indian Ocean. This result is expected due to the conformation of the territory, with the atolls creating sheltered areas. Nonetheless, it provides a first encouraging indication about the suitability of offshore platforms, including those for OTEC applications, to the site.

In order to establish the correlation between wind and waves predominant directions, the contributors to the energy spectrum should be analyzed separately. Because of the topography of the territory, characterized by mostly flat coral island at around 1 m above sea level, it can be hypothesized that complex local wind regimes are unlikely to exist. Despite that this cannot be demonstrated from global models, which struggle in resolving fine scale topography, also this observation provides positive indications about the feasibility of the OTEC platform installation.

The databases exploited in this work are selected because of their free availability in the public domain

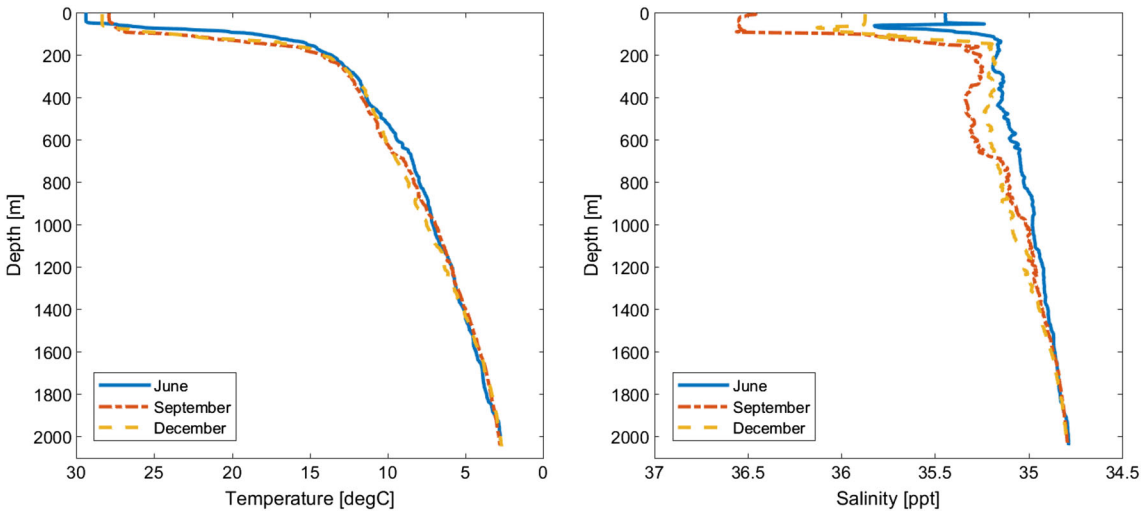

FIGURE 17 Temperature and salinity data for June, September, and December up to a depth of 2100 m [Colour figure can be viewed at wileyonlinelibrary.com]

and with the intent of covering as many of the metocean parameters as possible. These provide valuable information for the long-term characterization of the available resource and allow for an extreme event analysis. These data are produced by numerical simulation codes, and even if not accurate enough for commercial wave or wind projects, it represents a suitable alternative for preliminary assessment studies. However, these databases are all subject to different constraints in terms of spatial and temporal resolutions, as well as availability of data and kind of source provided. Although the ERA-Interim and WWIII wind and wave data are qualitatively compared with each other, data validation against buoys, satellites, scatterometers, or other instrumentation data remains the favorite option. The same principle applies to the data retrieved from the HYCOM database. However, preliminary validation of the data used in this work against results published in literature (as detailed in Section 2.1) allows to affirm with confidence that the values computed in the analysis are likely to be suitable for the extreme value and OTEC feasibility assessments.

Although not specifically related to this study, other limitations of global wave models like the ones used in this study may involve difficulties in modelling waves in points that are, for example, too close to the shore or with shallow waters. In other words, there is the risk that land masses and bathymetric features might not be properly resolved due to the low resolution of the model. In this case, model grid points close to land masses are likely to be less accurate.

In the investigated location, the 10- and 100-year return values are found to be relatively small in comparison with typical extreme values offshore infrastructures are designed for. When the extreme waves are analyzed by sector, those having higher return periods come from the western sectors, which seems counterintuitive because the atolls should provide shelter thus reducing the waves. Although it is unlikely that locally generated forcings develop into the most dominant extremes for an area, a possible reason for this oddity might be the effect of waves generated locally, as a results of the westerly winds found to be predominant in the analysis of wind resource, as opposed to the majority of the swell-generated waves coming mainly from southeast. A joint occurrence of possible energy period is provided for each sector. However, the final assessment should take into account not only the extreme values but also and especially the possible resonance of the device for specific values or combinations of wave height and period. For this reason, a response amplitude operator (RAO) analysis is needed in combination with the extreme analysis. Finally, despite this work focusing on the 1- to 100-year return values, extrapolation beyond these limits can be easily obtained with the same distributions produced (but with increased uncertainty).

Together with the return values of extreme events estimated from metocean data, the recurrence of extraordinary events, ie, tropical storms and cyclones, is assessed. Different databases, chosen among others because of their availability in the public domain, are consulted in order to extend the period of time investigated and retrieve information from different sources. Understandably, the major concerns for the design of the OTEC platform are related to the waves the cyclones can generate during their passage. According to the past tracked events, despite some differences in the consulted databases, it can be assessed that cyclones do not affect directly the location selected in this study nor in general the Maldives territory. Besides, their intensity rarely reaches levels that may affect the integrity of the OTEC infrastructure. However, the possibility of storm generated waves as a consequence of a cyclone, which might exceed the return values provided in this analysis, still persists. Some reassurance in this sense is given by the fact that, according to this study, cyclones and extreme waves have discording main directionality. Nonetheless, it must be remembered that cyclone-generated waves radiate from their site of generation and are not therefore constrained in their reach by the path of the cyclone. In this regard, a comparison between recorded tropical storms and the highest values in the downloaded metocean data would be valuable in order to gain confidence in the extreme value estimations. However, due to their parametrization and intended use, models on a global scale might have limitations in capturing the formation and evolution of cyclones and hurricanes. Regional climate models, allowing for a higher resolution, generally have major capability in predicting and simulating tropical cyclones and could therefore be used to this end. In alternative, a more thorough approach would consist in assessing the performance of the global models used to simulate TRS in the specific region of interest. A review of parametric relations to model the wave field in tropical cyclones is provided in Young.[50]

The results of the CTD measurements on temperature variations, in combination with the salinity profiles and weather and climate information provided above, also supports the expectation that this location is suitable for an OTEC platform. Assuming a device capacity of 1.5 MW and a capacity factor of 90%,[51] an energy production of 11.8 GWh/year can be reached. However, the data presented here should be further verified by in situ measurements to assess eventual differences against the available CTD data. Also, samples at greater depths and for extended period of times (in order to guarantee sufficient

temporal representativeness) would increase confidence in the assessment.

According to these characterizations, due to the sufficiently small metocean and extreme values, a spread mooring system is the most indicated for an OTEC platform to be installed in the Maldives. This configuration is cheaper and easier to install and maintain with respect to others, eg, the turret system previously considered as another suitable alternatives. In addition, the results of this metocean assessment will allow operators to calculate the required specifications of the mooring system, in terms of, eg, lines dimension and minimum breaking load. In this case, since the current speed values provided refer to the surface, a vertical current profile must be created using these as an upper limit. This provides a useful approximation of the oceanic currents throughout the water column, which allows for the calculation of the loads across the mooring lines. The main limitation of this approach is the uniform directionality of the currents. In other words, it is neglected that different water masses at different depths could be flowing in different directions.

With regard to the orientation of the platform, the outcomes of this study will allow load testing for different configurations, taking into account all the environmental conditions. As a result, the configuration with the narrow ends of the platform positioned at southeast and northeast respectively is found to be the most suitable orientation of the device.

5 | CONCLUSIONS

This paper provides a feasibility assessment of OTEC applications in the Maldives based on the characterization of the meteorological resource and an analysis of the extreme events. Temperature, salinity, wind, wave, and current data are collected from publicly available databases exploiting global climate models. Their distributions are analyzed in order to extrapolate useful information for OTEC and other marine renewable energy developers.

An extreme analysis provides return values for wind speeds and significant wave height, along with representative energy periods. These values inform prediction of the loads that an offshore platform should withstand. For instance, using the metocean conditions found in this study and a numerical model of the OTEC plant implemented in Orcaflex, the tension on the mooring lines as a result of the wave, wind, and current loads is found to reach a maximum of around 1000 kN. The maximum mooring line tension can be used to define the minimum breaking loads of the chain and rope, which in turn is used to select the appropriate thickness of these components.

Further analysis, showing the southwestern sectors as those from which extreme events are more likely to originate, provides the directionality of these extremes to support alignment and positioning of infrastructure. The final orientation of the OTEC device is chosen at 135°, with north being zero.

Analysis of past tropical storms indicates that the risk from tropical cyclones at the selected location is low, with 22 cyclones of moderate intensity registered in the past 89 years.

Future work will consist in further validation of the metocean data used for this study would benefit the analysis. This could be achieved by means of comparison against data collected in the area of interest using appropriate instruments. Similarly, further socioeconomic and environmental considerations, eg, water availability and sea level rise, are needed in order to assess the viability of ocean renewable projects in the Maldives archipelago.[2,42] Finally, future investigation will consist in determining the structural specifications of the OTEC platform and grid connection systems according to the values provided in this work and other engineering constraints. This information will then be used to produce a complete study on the potential impact and expenses of the OTEC plant, in order to aid decisions on the viability of the project.

Nonetheless, the results shown in this work, such as a ΔT of 24°C and 100-year H_S of 4.5 m, bode well for the future installation and deployment of offshore systems. These characterizations provide valuable information on the structural and directional requirements of the OTEC platform. Valuable information and a series of considerations are provided for both the design of the offshore platform and its mooring system, thus reducing the risk and cost of overengineering all structural components.

ACKNOWLEDGEMENTS

The authors would like to express their gratitude to the Editor and the anonymous reviewers for their comments and suggestions. The content and structure of the paper has significantly improved as a consequence of the review process.

CONFLICT OF INTEREST

The authors declare no conflict of interest. The funders had no role in the design of the study; in the collection, analyses, or interpretation of data; in the writing of the manuscript; or in the decision to publish the results.

FUNDING INFORMATION

This research was funded by the European Union under the European Regional Development Funding (ERDF) Marine-i, grant number 05R16P00381.

ORCID

Giovanni Rinaldi https://orcid.org/0000-0001-6296-4911
Ed Mackay https://orcid.org/0000-0001-7121-4231
Ian Ashton https://orcid.org/0000-0001-8744-4760
Lars Johanning http://orcid.org/0000-0002-3792-3373

REFERENCES

1. Maldives Energy Authority, Maldives Energy Supply & Demand Survey, Gov. Maldives. 2012.
2. Owen A, Kruijsen J, Turner N, Wright K. Marine energy in the Maldives, Aberdeen, 2011.
3. Elliott D, Schwartz M, Scott G, Haymes S, Heimiller D, George R. Wind energy resource atlas of Sri Lanka and the Maldives, 2003.
4. Contestabile P, Di Lauro E, Galli P, Corselli C, Vicinanza D. Offshore wind and wave energy assessment around malè and Magoodhoo Island (Maldives). *Sustain*. 2017;9(4):613. https://doi.org/10.3390/su9040613
5. Pérez-collazo C, Greaves D, Iglesias G. A review of combined wave and offshore wind energy. *Renew Sustain Energy Rev*. 2015;42:141-153. https://doi.org/10.1016/j.rser.2014.09.032
6. Richards WE, Vadus JR. Ocean thermal energy conversion: technology development. *Ocean Manag*. 1981;7(1-4):327-352.
7. Faizal M, Ra M. Experimental studies on a closed cycle demonstration OTEC plant working on small temperature difference. *Renew Energy*. 2013;51:234-240. https://doi.org/10.1016/j.renene.2012.09.041
8. Tanner D. Ocean thermal energy conversion: current overview and future outlook. *Renew Energy*. 1995;6(3):367-373.
9. Devault DA, Péné-annette A. Analysis of the environmental issues concerning the deployment of an OTEC power plant in Martinique. *Environ Sci Pollut Res*. 2017;24(33):25582-25601. https://doi.org/10.1007/s11356-017-8749-3
10. Cassone G, Chille D, Foti C, Giuffre O, Ponterio RC. Stability of hydrolytic arsenic species in aqueous solutions: As 3+ vs. As 5+. *Phys Chem Chem Phys*. 2018;20:23272-23280. https://doi.org/10.1039/c8cp04320e
11. Nihous G. A preliminary investigation of the effect of ocean thermal energy conversion (OTEC) effluent discharge options on Global OTEC Resources. *J Mar Sci Eng*. 2018;6(1):25. https://doi.org/10.3390/jmse6010025
12. Jia Y, Nihous K, Gérard C. Rajagopalan, An evaluation of the large-scale implementation of ocean thermal energy conversion (OTEC) using an ocean general circulation model with low-complexity atmospheric feedback effects. *J Mar Sci Eng*. 2018;6(1):12. https://doi.org/10.3390/jmse6010012
13. Worrall N. Analysis of providing affordable electricity supply for the outer islands in the Maldives, 2006.
14. Wang CM, Yee AA, Krock H, Tay ZY. Research and developments on ocean thermal energy conversion. *IES J Part A Civ Struct Eng*. 2011;4:41-52. https://doi.org/10.1080/19373260.2011.543606
15. National Oceanic and Atmospheric Administration (NOAA), Geospatial data and services, (n.d.). https://maps.ngdc.noaa.gov/viewers/bathymetry/ (accessed June 26, 2019).
16. Greaves D, Conley D, Leeney RH, et al. The SOWFIA Project: streamlining of ocean wave farms impact assessment, 2014. https://ec.europa.eu/energy/intelligent/projects/en/projects/sowfia.
17. Dee DP, Uppala SM, Simmons AJ, et al. The ERA-Interim reanalysis: configuration and performance of the data assimilation system. *Q J Roy Meteorol Soc*. 2011;137:553-597. https://doi.org/10.1002/qj.828
18. HYCOM, Hybrid Coordinate Ocean Model, (2018). https://www.hycom.org/hycom/overview (accessed January 28, 2019).
19. http://sowfia.hidromod.com/PivotMapViewer/, (2018).
20. ERA-Interim dataset, (2018). https://www.ecmwf.int/en/forecasts/datasets/reanalysis-datasets/era-interim (accessed November 18, 2018).
21. HYCOM + NCODA Global 1/12° Reanalysis, (n.d.). https://www.hycom.org/dataserver/gofs-3pt1/reanalysis (accessed November 8, 2018).
22. Chassignet EP, Hurlburt HE, Smedstad OM, et al. The HYCOM (HYbrid Coordinate Ocean Model) data assimilative system. *J Mar Syst*. 2007;65(1-4):60-83. https://doi.org/10.1016/j.jmarsys.2005.09.016
23. Shanas PR, Kumar VS. Comparison of ERA-Interim waves with buoy data in the eastern Arabian Sea during high waves. *Indian J Geo-Marine Sci*. 2014;43:1343-1346.
24. Sangalugeme C, Luhunga P, Kijazi A, Kabelwa H. Validation of operational WAVEWATCH III Wave Model Against Satellite Altimetry Data Over South West Indian Ocean Off-Coast of Tanzania. *Appl Phys Res*. 2018;10(4):55-65. https://doi.org/10.5539/apr.v10n4p55
25. Lüdmann T, Kalvelage C, Betzler C, Fürstenau J, Hübscher C. The Maldives, a giant isolated carbonate platform dominated by bottom currents. *Mar Pet Geol*. 2013;43:326-340. https://doi.org/10.1016/j.marpetgeo.2013.01.004
26. Rao LVG, Ram PS. Upper ocean physical processes in the Tropical Indian Ocean, Visakhapatnam, 2005.
27. Tomczak M, Godfrey JS. *Regional Oceanography: An Introduction*. Amsterdam: Pergamon; 1994 doi: https://doi.org/10.1016/B978-0-08-041021-0.50005-9.
28. Shankar D, Vinayachandran PN, Unnikrishnan AS. The monsoon currents in the north Indian Ocean. *Prog Oceanogr*. 2002;52(1):63-120. https://doi.org/10.1016/S0079-6611(02)00024-1
29. Coles S. *An Introduction to Statistical Modeling of Extreme Values*. Bristol: Springer; 2001 doi: https://doi.org/10.1007/978-1-4471-3675-0.
30. Palutikof JP, Brabson BB, Lister DH, Adcock ST. A review of methods to calculate extreme wind speeds. *Meteorol Appl*. 1999;6(2):119-132. https://doi.org/10.1017/S1350482799001103

31. van den Brink HW, Können GP, Opsteegh JD, van Oldenborgh GJ, Burgers G. Estimating return periods of extreme events from ECMWF seasonal forecast ensembles. *Int J Climatol*. 2005;25(10):1345-1354. https://doi.org/10.1002/joc.1155
32. Soukissian TH, Kalantzi GD. Extreme value analysis methods used for wave prediction, in: Int. Offshore Polar Eng. Conf., San Francisco, California, USA, 2006: pp. 10–17.
33. Mackay EBL. *Resource assessment for wave energy*. Exeter, UK: Elsevier Ltd.; 2012 doi: https://doi.org/10.1016/B978-0-08-087872-0.00803-9.
34. Bezak N, Brilly M, Šraj M. Comparison between the peaks-over-threshold method and the annual maximum method for flood frequency analysis. *Hydrol Sci J*. 2014;59(5):959-977. https://doi.org/10.1080/02626667.2013.831174
35. Van Vledder G, Goda Y, Hawkes P, et al. *Case studies of extreme wave analysis: a comparative analysis, in: Ocean Wave Meas*. New York: Anal. ASCE; 1993:978-992.
36. Guedes Soares C, Scotto M. Modelling uncertainty of long-term predictions of significant wave height. *Ocean Eng*. 2001;28(3):329-342.
37. Jonathan P, Ewans K. Statistical modelling of extreme ocean environments for marine design: A review. *Ocean Eng*. 2013;62:91-109. https://doi.org/10.1016/j.oceaneng.2013.01.004
38. Mackay E, Johanning L. Long-term distributions of individual wave and crest heights. *Ocean Eng*. 2018;165:164-183. https://doi.org/10.1016/j.oceaneng.2018.07.047
39. Soukissian TH, Kalantzi GD, Karagali I. De-clustering of Hs-time series for applying the peaks-over-threshold method, in: Int. Offshore Polar Eng. Conf., San Francisco, California, USA, 2006.
40. Zhang J. Likelihood moment estimation for the generalized pareto distribution. *Aust New Zeal J Stat*. 2007;49(1):69-77. https://doi.org/10.1111/j.1467-842X.2006.00464.x
41. Faltinsen O. *Sea loads on ships and offshore structures*. Cambridge, UK: Cambridge university press; 1993.
42. Karthikheyan TC. Environmental Challenges for Maldives. *South Asian Surv*. 2010;17(2):343-351. https://doi.org/10.1177/097152311201700210
43. Bimal PK, Rashid H. Tropical cyclones and storm surges, in: Clim. Hazards Coast. Bangladesh, 2017: pp. 35–81.
44. European Centre for Medium-Range Weather Forecasts, ECMWF tropical cyclone track, (2019). https://www.ecmwf.int/en/forecasts/charts/tcyclone/ (accessed January 28, 2019).
45. World Meterorological Organization, Terminologies and acronyms used in the region of Western North Pacific and the South China Sea by the typhoon Committee Members, 2019. http://severe.worldweather.wmo.int/tc/wnp/acronyms.html (accessed January 28, 2019).
46. Knapp KR, Kruk MC, Levinson DH, Diamond HJ, Neumann CJ. The International Best Track Archive for Climate Stewardship (IBTrACS): unifying tropical cyclone best track data. *Bull Am Meteorol Soc*. 2010;91:363-376. https://doi.org/10.1175/2009BAMS2755.1
47. Kourafalou VH, Peng G, Kang H, Hogan PJ, Smedstad OM, Weisberg RH. Evaluation of global ocean data assimilation experiment products on south florida nested simulations with the hybrid coordinate ocean model. *Ocean Dyn*. 2009;59(1):47-66. https://doi.org/10.1007/s10236-008-0160-7
48. BODC, British Oceanographic Data Centre, (2018). https://www.bodc.ac.uk/ (accessed December 20, 2018).
49. eWOCE, World Ocean Circulation Experiment, (2018). http://www.ewoce.org/ (accessed December 20, 2018).
50. Young IR. A review of parametric descriptions of tropical cyclone wind-wave generation. *Atmosphere (Basel)*. 2017;8:194. https://doi.org/10.3390/atmos8100194
51. International Renewable Energy Agency (IRENA), Ocean thermal energy conversion—technology brief, (2014).

SUPPORTING INFORMATION

Additional supporting information may be found online in the Supporting Information section at the end of the article.

How to cite this article: Rinaldi G, Crossley G, Mackay E, et al. Assessment of extreme and metocean conditions in the Maldives for OTEC applications. *Int J Energy Res*. 2019. https://doi.org/10.1002/er.4762

APPENDIX A.

RETURN VALUES AND CONFIDENCE INTERVALS

All the extreme values provided in this work have been estimated within a 95% confidence interval, using the bootstrap technique.[33,38] In this appendix, the confidence bounds are reported for each of the return value provided.

TABLE A1 Directional extreme values for significant wave height, together with lower and higher bounds (confidence intervals)

	1-year Return Value			10-year Return Value			100-year Return Value		
Sector	LB	CI	HB	LB	CI	HB	LB	CI	HB
N	-	-	-	-	-	-	-	-	-
NE	1.31	1.34	1.36	1.89	2.07	2.24	2.08	2.47	2.65
E	1.78	1.83	1.90	2.28	2.44	2.56	2.51	2.82	3.77
SE	1.75	1.81	1.84	2.24	2.37	2.57	2.43	2.84	3.23
S	2.01	2.03	2.05	2.38	2.58	2.80	2.67	3.32	4.72
SW	1.84	1.89	1.96	2.70	2.95	3.14	2.90	3.41	3.61
W	2.57	2.64	2.72	3.07	3.45	3.80	3.26	4.22	5.02
NW	-	-	-	-	-	-	-	-	-

Abbreviations: CI; 95% confidence interval; HB, higher bound (97.5% quantile); LB, lower bound (2.5% quantile).

TABLE A2 Directional extreme values for wind speed, together with lower and higher bounds (confidence intervals)

	1-year Return Value			10-year Return Value			100-year Return Value		
Sector	LB	CI	HB	LB	CI	HB	LB	CI	HB
N	6.49	6.70	6.99	8.13	8.76	9.07	8.48	9.53	9.82
NE	9.05	9.28	9.56	10.69	11.72	12.58	11.17	13.65	15.33
E	8.76	9.01	9.33	11.15	12.46	13.92	11.69	15.85	19.45
SE	0.60	0.91	2.07	7.67	9.03	10.35	8.39	12.47	13.40
S	4.76	5.14	5.40	8.12	8.68	9.13	8.98	9.84	10.02
SW	11.08	11.48	11.89	13.50	15.19	16.24	14.15	17.70	19.62
W	12.54	12.87	13.20	13.81	15.51	16.24	14.12	17.33	18.55
NW	9.56	9.90	10.32	11.88	12.96	13.55	12.45	14.33	14.91

Abbreviations: CI; 95% confidence interval; HB, higher bound (97.5% quantile); LB, lower bound (2.5% quantile).

TABLE A3 Directional extreme values for current speed, together with lower and higher bounds (confidence intervals)

	1-year Return Value			10-year Return Value			100-year Return Value		
Sector	LB	CI	HB	LB	CI	HB	LB	CI	HB
N	0.49	0.56	0.62	0.61	0.74	0.76	0.64	0.78	0.84
NE	0.57	0.68	0.78	0.64	0.93	1.01	0.65	1.03	1.17
E	0.74	0.82	0.87	0.79	0.94	0.98	0.80	0.99	1.04
SE	1.03	1.19	1.26	1.09	1.36	1.46	1.10	1.45	1.58
S	0.68	0.79	0.88	0.77	1.01	1.07	0.79	1.08	1.20
SW	0.66	0.84	1.06	0.79	1.40	1.90	0.84	1.93	3.50
W	1.15	1.32	1.45	1.28	1.65	1.84	1.32	1.82	2.10
NW	0.88	1.05	1.20	1.00	1.38	1.53	1.03	1.53	1.74

Abbreviations: CI; 95% confidence interval; HB, higher bound (97.5% quantile); LB, lower bound (2.5% quantile).